DOI 10.1007/s10946-022-10063-0
Journal of Russian Laser Research, Volume 43, Number 3, May, 2022

STUDY ON REAL-TIME MEASUREMENT OF FEMTOSECOND LASER PULSE WIDTH BASED ON NONCOLLINEAR SECOND-HARMONIC GENERATION EFFECT

Yashuai Yang, Yongliang Li,* Chi Wang, and Xiaoting Sun

The School of Opto-electronics Engineering
Changchun University of Science and Technology
Changchun 130022, Jilin, China

*Corresponding author e-mail: liyongliang3@126.com

Abstract

We propose an autocorrelator based on noncollinear second-harmonic generation effect and a pulse-width measurement program written by LabVIEW software providing online analysis, process measurement data, and real-time display of femtosecond laser pulse width. The autocorrelator is calibrated by the online self-calibration method, and an average accuracy of 1.049 fs/pixel is obtained. On this basis, we perform a verification test on a laser pulse with a center wavelength of 800 nm and a pulse width of about 90 fs; the obtained Gaussian pulse width is 95.3 fs. The test results show that the autocorrelation device can realize real-time and accurate measurement of laser pulse width within 100 fs.

Keywords: noncollinear second-harmonic generation effect, femtosecond laser, pulse-width measurement, autocorrelation.

1. Introduction

The pulse width is an important indicator to evaluate the time domain characteristics of pulses. The laser pulse width has undergone several stages, such as milliseconds (10^{-3} s), microseconds (10^{-6} s), nanoseconds (10^{-9} s), picoseconds (10^{-12} s), femtosecond (10^{-15} s), and attosecond (10^{-18} s). At present, attosecond pulse is in the exploration stage [1–3]. Femtosecond laser, as a light source with ultrafast pulse and high peak power, is widely used in ranging [4, 5], communication [6, 7], medicine [8, 9], biology [10, 11], chemistry [12], precision machining [13, 14], and other fields. Therefore, it is of great significance to measure the pulse width accurately, rapidly, and conveniently for the research and application of femtosecond lasers.

At present, the measurement methods of ultrafast-laser pulse width mainly include direct and indirect measurement methods. The direct measurement methods generally use fringe cameras to detect the length of the fringe to calculate the pulse width to be measured, and the incident pulse waveform is simultaneously obtained according to the fringe envelope [15–17]. This method can obtain the pulse width and waveform to be measured intuitively and accurately. However, the current time limit resolution of electronic detection technology is in the order of picoseconds. For pulses with a pulse width of <100 fs, indirect measurement methods are often used to measure the pulse width. The measurement methods mainly include the two-photon fluorescence method [18,19], the second-harmonic generation autocorrelation method [20–24], the third-order autocorrelation method [25,26], the frequency-resolved optical gating

Manuscript submitted by the authors in English on June 17, 2021.

method [27,28], spectral phase interferometry for direct electric-field reconstruction method [29,30], etc. Due to its simple structure and high resolution, the second-harmonic generation autocorrelation method is the most commonly used and currently the most advantageous measurement method. However, the second-harmonic generation autocorrelation method generally measures the second-harmonic generation signal through CCD or photomultiplier tube and the data is analyzed off-line later on. Because the pulse-width information cannot be obtained in real time, the pulse-width monitoring and application of femtosecond lasers are restricted.

Compared with the previous scheme [31], (1) we use only four mirrors to simplify the design of a single autocorrelator; (2) we employ two mirrors to adjust two pulses independently to focus in the nonlinear crystal, which reduces the debugging difficulty when using one mirror to adjust two pulses at the same time; (3) we use a slit to block the fundamental frequency signal, which not only avoids the damage of the CCD caused by the fundamental frequency signal of the peak power but also simplifies the process of eliminating the fundamental light in the pulse-width measurement program. In addition, we use another linear CCD with smaller pixel to measure the second-harmonic signal and carry out the secondary development of the CCD camera. We use LabVIEW software to transfer the light intensity value of each pixel measured by linear CCD into LabVIEW executable program in the form of calling sub-VI to process the data results twice.

In this paper, we describe the principle of self-calibration and the process of online self-calibration in more detail. Due to the smaller pixel linear CCD, the average accuracy of a single pixel is 1.049 fs. Using such the autocorrelator, we measure online the laser pulse with a central wavelength of 800 nm and a pulse width of about 90 fs; the measured Gaussian pulse width is 95.3 fs.

2. Measuring Principle

According to the speed of light, the pulse space duration of 1 fs is 0.3 μm. This distance can be resolved by a precision displacement platform. Therefore, the time width of the femtosecond laser pulse can be converted into the space length for measurement. The measurement principle of the noncollinear second-harmonic generation autocorrelator is shown in Fig. 1. Two identical pulses intersect at a certain angle in the crystal, and one of the pulses is delayed by a displacement device. The second-harmonic generation signal is emitted along the symmetry axis of the angle between the two pulses, and the second-harmonic generation signal is received by the CCD camera. The spatial width of the second-harmonic generation signal is proportional to the laser pulse width [22],

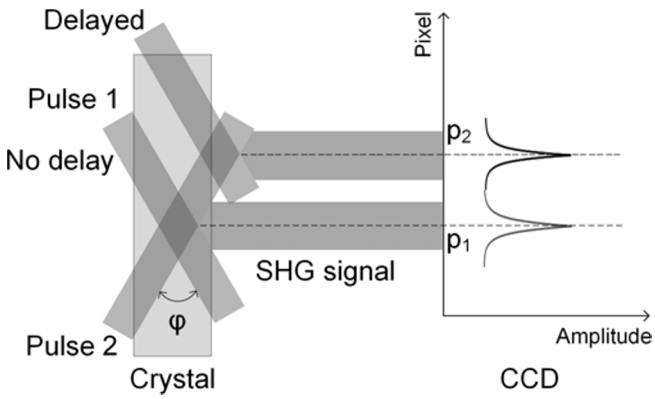

Fig. 1. Schematic diagram of noncollinear second-harmonic generation autocorrelator.

$$\Delta\omega = \frac{\tau_p v_g}{\sin(\varphi/2)}, \tag{1}$$

where $\Delta\omega$ is the space width of the second-harmonic generation signal, τ_p is the laser pulse width, v_g is the group velocity of light in the crystal, and φ is the angle between the two pulses.

Since it is not easy to accurately determine the angle φ, a self-calibration method is used to calibrate the autocorrelator. The self-calibration process is as follows: move two mutually perpendicular mirrors through the displacement platform to realize the delay of a pulse. As the overlapping position of the two pulses in the crystal changes, the second-harmonic generation signals are shifted on the CCD camera. When there is no delay, the micrometer reading of displacement platform is x_1, and the number of the pixel corresponding to the second-harmonic generation signal peak is p_1. After providing the time delay, the micrometer reading of the displacement platform is x_2, and the number of the pixel corresponding to the peak of the second-harmonic generation signal is p_2. The delay time is obtained by the double moving distance of the displacement platform $2|x_2 - x_1|$ divided by the speed of light c. The delay time is divided by the offset of the pixel position $|p_2 - p_1|$ to obtain the time scale corresponding to the unit pixel of the CCD. The number of pixels P included in the full width at half maximum of the second-harmonic generation signal is multiplied by the time scale corresponding to the unit pixel to obtain the width of the second-harmonic generation signal. The second-harmonic signal width is divided by the waveform coefficient K of the pulse to be measured, and the laser pulse width is calculated. The Gaussian pulse coefficient is 1.414, and the hyperbolic secant pulse coefficient is 1.543. Therefore, the femtosecond-laser pulse width can be measured as follows:

$$\tau = \frac{1}{K} \cdot \frac{2|x_2 - x_1|}{p_2 - p_1} \cdot 1c \cdot P. \tag{2}$$

3. Measuring Device

The noncollinear second-harmonic generation autocorrelator device is shown in Fig. 2. The femtosecond laser pulse to be measured first passes through diaphragm 1 to convert the pulse into a standard pulse, and then passes through diaphragm 2 to ensure that the pulse is collimated and incident. The standard pulse is divided into two identical pulses by a 50:50 beam splitter. One pulse passes through the delay device composed of mirrors M1 and M2 on the precision displacement platform. The stroke of the precision displacement platform is 20 mm and the sensitivity is better than 2 μm. The other pulse passes through mirrors M3 and M4, and the two pulses are focused on the BBO crystal to generate the second-harmonic generation signal. The BBO crystal is fixed by an optical adjustment frame that can be precisely rotated. The optical paths of the two pulses from the beam splitter to the BBO crystal are basically the same. The slit shields the fundamental frequency signal, and the second-harmonic generation signal is finally received by the CCD. The measurement results are displayed in the software in real time. The CCD model is BLU0708M30, which contains 5150 pixels. The size of a

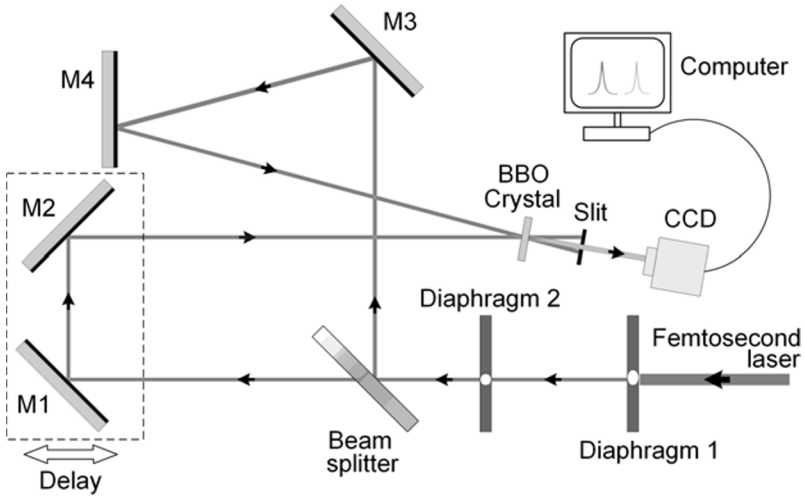

Fig. 2. Installation diagram of noncollinear second-harmonic generation autocorrelator.

single pixel is 7×7 μm, and the wavelength response range is 300- 1100 nm. The camera is connected to a computer through a USB 2.0 high-speed bus interface without a discrete capture card.

The optical components used in the experimental device are matched with a 800 nm center wavelength of the femtosecond laser to be measured. In addition, because the measured femtosecond laser pulse has a certain spectral width, the pulse width becomes wider when passing through some optical elements. Therefore, the autocorrelator uses low-dispersion components, where the thickness of the beam splitter BS is 0.15 mm, M1–M4 are all gold-coated mirrors, and the BBO size is 10×10×0.4 mm.

4. Testing Process and Analysis of Results

4.1. Testing Process

In this study, we transfer the CCD measurement data into the LabVIEW executable program in the form of LabVIEW calling sub VI for data acquisition and analysis. A self-written pulse-width measurement program is used to measure the femtosecond laser pulse output by a Ti:Sapphire laser oscillator (Coherent, Mira-900) with a center wavelength of 800 nm, a pulse-width of about 90 fs, and a repetition rate of 76 MHz. We use an InGaAs fiber spectrometer (StellarNet, BW-UVN-50) to measure the spectrum of the laser pulse. The measured spectrum is shown in Fig. 3, with a center wavelength of 799.77 nm and a spectral width of 11.2 nm.

Before the test, first adjust the light path using the guiding light to ensure that the two pulses are transmitted at the same height. Second, ensure that all the light spots are at the center of the mirrors, and finally ensure that the two pulses intersect at the BBO crystal. After adjusting the optical path, the femtosecond laser to be measured is placed on the coaxial position with the guiding light.

Before measuring the pulse width, we first adjust the power of the femtosecond laser to be measured to 800 mW to ensure that the reflectors, beam splitter, BBO crystal, and CCD camera in the autocorrelator device work within the safety threshold. At the same time, a power meter is used to measure the power of the two pulses. The power of the delayed beam is 382 mW and the power of the undelayed beam is 366 mW. By rotating the angle of the BBO crystal to achieve a phase matching state, a blue–

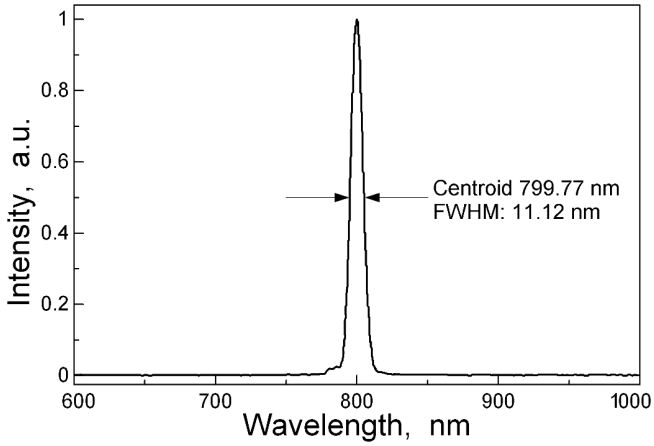

Fig. 3. The spectrum of the laser pulse to be measured.

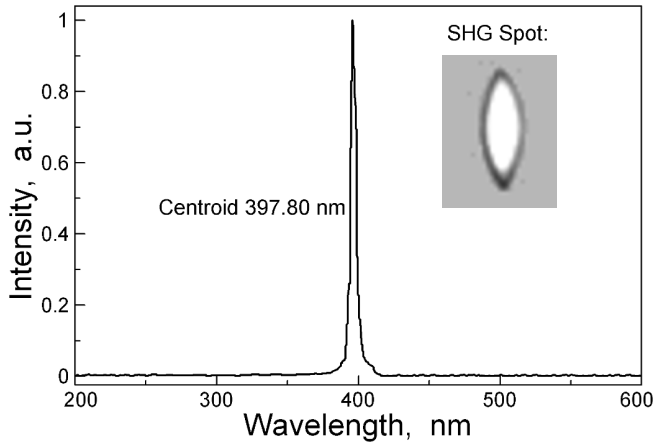

Fig. 4. Second-harmonic generation signal spectrum and spot diagram.

violet second-harmonic-generation signal will be observed behind the crystal. By adjusting the manual displacement platform to provide time delay, the second-harmonic generation signal can be observed, when the micrometer reading is between 9.842 and 10.312 mm. Finally, we adjust the size of the slit to shield the fundamental-frequency signal, and adjust the position of the CCD camera to make the second-harmonic light signal displayed near the middle of the software interface. We test the spectrum of the second-harmonic generation signal. The spectrum is shown in Fig. 4, and the central wavelength is 397.80 nm; the second-harmonic generation spot is shown in the upper right corner.

In order to reduce the measurement error as much as possible, two relatively distant coherent points are selected for calibration. When moving the displacement platform, the second-harmonic generation signal will move to left or right on the software interface. At the first measurement point, the pixel number, where the wave crest is located, is 1774. We input the reading of the displacement platform micrometer at this time into the measurement program, which is 10.168 mm. At the second measurement point, the pixel, where the wave crest is located, is 1504. We input the reading of the displacement platform micrometer at this time into the measurement program, which is 10.252 mm. After completing the online self-calibration, the measurement program shows that the average single-pixel accuracy of this experiment is 1.049 fs. The self-calibration result is shown in Fig. 5.

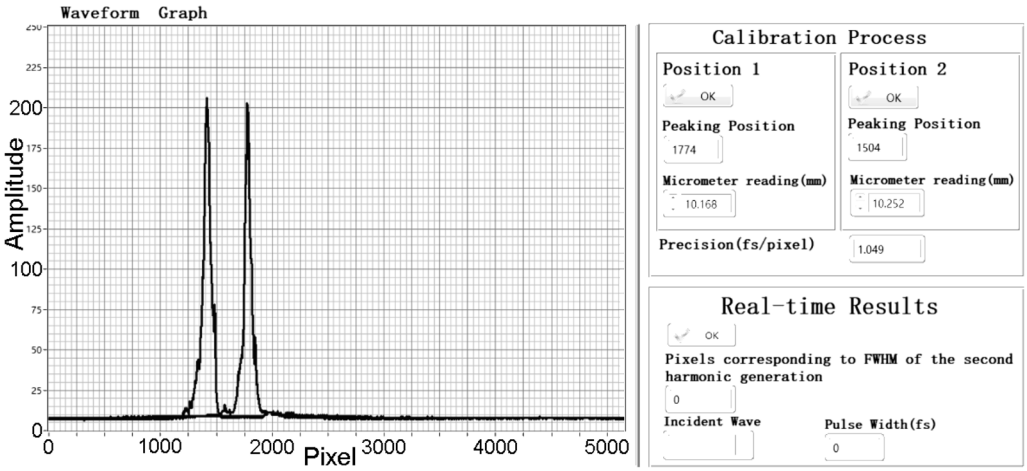

Fig. 5. The result of on-line self-calibration.

5. Analysis of the Results

Because we use LabVIEW software to directly transfer the light intensity value of each pixel into the LabVIEW executable program by calling sub-VI, the waveform of the second-harmonic signal will be displayed in real time on the software interface. The number of pixels corresponding to the full width at half maximum of the second-harmonic signal and the Gaussian pulse width of the femtosecond laser can be obtained in 1 s. By fine tuning the displacement platform, the number of pixels corresponding to the full width at half maximum of the second-harmonic generation signal displayed in real time and the Gaussian pulse width of the femtosecond laser produced small fluctuations. During the adjustment process, the minimum number of pixels corresponding to the full width at half maximum of the second-harmonic generation signal is 64.2, and the Gaussian pulse width of the femtosecond laser is 95.3 fs. The test results are shown in Fig. 6.

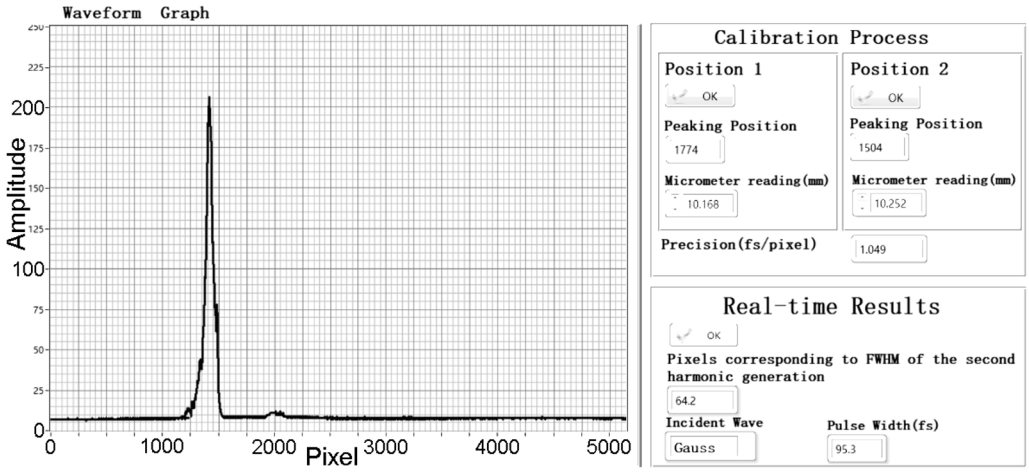

Fig. 6. Test results of the pulse width.

The measured Gaussian pulse width of femtosecond laser is 95.3 fs, which is consistent with the actual pulse width. However, due to the certain linewidth of the femtosecond laser pulse, the dispersion effect cannot be avoided when the laser pulse passes through the splitter and nonlinear crystal. As a result, the measured pulse width is slightly larger than the actual pulse width.

6. Conclusions

In this paper, we built a single autocorrelator based on noncollinear second-harmonic generation effect for measuring the pulse width of femtosecond laser, and write a pulse-width measurement program based on LabVIEW software, which can realize online analysis and processing of measurement data along with real-time display. In the test, we used the online self-calibration method to obtain an average accuracy of 1.049 fs/pixel. We employed this device to test a laser pulse with a center wavelength of 800 nm and a pulse width of about 90 fs; the measured Gaussian pulse width is 95.3 fs. The test results show that the device can accurately measure the pulse width of femtosecond laser in real time. We solved the problem that the traditional autocorrelation instruments cannot monitor the femtosecond laser pulse width in real time. It can provide practical testing methods and performance monitoring guarantee for the development and application of femtosecond lasers.

Acknowledgments

The authors acknowledged the support provided by the National Natural Science Foundation of China under Grant No. 62075018 and People's Government of Jilin Province under Grant Nos. 20191102009YY and 20200403018SF.

References

1. A. V. Mitrofanov, D. A. Sidorov-Biryukov, P. B. Glek, et al., *Opt. Lett.*, **45**, 750 (2020).
2. S. Zhou, Y. Yang, D. Ding, et al., *Opt. Commun.*, **370**, 294 (2016).
3. J. D. Sadler, M. Sliwa, T. Miller, et al., *High Energy Density Phys.*, **23**, 212 (2017).

4. H. Cao, Y. Song, Y. Li, et al., *Appl. Sci.*, **8**, 1625 (2018).
5. Z. Shen, T. Liu, H. Liu, et al., *Optik*, **125**, 5884 (2014).
6. H. M. Alyami, V. M. Becerra, and S. Hadjiloucas, *J. Phys. Conf. Ser.*, **472**, 012009 (2013).
7. A. M. Weiner, *Opt. Quantum Electron.*, **32**, 473 (2000).
8. M. Terakawa, T. Mitsuhashi, T. Shinohara, et al., *Opt. Express*, **21**, 12604 (2013).
9. B. Luca, P. Gianni, and V. Paola, *J. Ophthalmol.*, **2012**, 264590 (2012).
10. D. S. Sitnikov, M. L. Semenova, M. A. Filatov, et al., *High Temp.*, **54**, 1 (2015).
11. C. V. Gabel, *Contemp. Phys.*, **49**, 391 (2008).
12. Y. A. Gauduel, *J. Phys. Conf. Ser.*, **373**, 012012 (2016).
13. W. Nathan, J. Jason, and S. Jeff, *Opt. Commun.*, **430**, 352 (2018).
14. X. W. Cao, Q. D. Chen, F. Hua, et al., *Nanomaterials*, **8**, 287 (2018).
15. D. J. Bradley, B. Liddy, and W. E. Sleat, *Opt. Commun.*, **2**, 391 (1971).
16. P. Gallant, P. Forget, F. Dorchies, et al., *Rev. Sci. Instrum.*, **71**, 3627 (2000).
17. N. H. Schiller and R. R. Alfano, *Opt. Commun.*, **35**, 451 (1980).
18. E. Z. Chong, T. F. Watson, and F. Festy, *Appl. Phys. Lett.*, **105**, 658 (2014).
19. J. Chen, W. Xia, and M. Wang, *J. Appl. Phys.*, **121**, 223103 (2017).
20. H. N. Kim, S. H. Park, K. N. Kim, et al., *J. Opt. Soc. Korea*, **18**, 382 (2014).
21. H. Mashiko, A. Suda, and K. Midorikawa, *Appl. Phys. B*, **87**, 221 (2007).
22. M. Raghuramaiah, A. K. Sharma, P. A. Naik, et al., *Sadhana*, **26**, 603 (2001).
23. M. Narimousa, M. Sabaeian, S. M. M. Ghahfarrokhi, et al., *Appl. Opt.*, **57**, 5011 (2018).
24. A. Farag and A. Nause, *Instrum. Exp. Tech.*, **63**, 547 (2020).
25. T. Feurer, S. Niedermeier, and R. Sauerbrey, *Appl. Phys. B*, **66**, 163 (1998).
26. S. Tao, B. Wang, S. Zhong, et al., *Optik*, **124**, 3461 (2013).
27. T. Yoshinari, I. Tomoko, K. Yuichiro, et al., *Appl. Sci.*, **5**, 136 (2015).
28. Y. Nakano and T. Imasaka, *Appl. Phys. B*, **123**, 157 (2017).
29. W. Tawfik, *J. Nonlinear Opt. Phys. Mater.*, **25**, 1550040 (2015).
30. A. Trisorio, S. Grabielle, M. Divall, et al., *Opt. Lett.*, **37**, 2892 (2012).
31. X. Sun, Y. Li, and Y. Yang, *J. Russ. Laser Res.*, **42**, 226 (2021).